

Nonlinear Flight Control Design of a Combat Flying Wing with High Aspect-ratio

Wang Lei

School of Aeronautic Science and Engineering
Beihang University
Beijing, China
wolsur@163.com

Wang Lixin

School of Aeronautic Science and Engineering
Beihang University
Beijing, China
bhu_wlx@tom.com

Abstract—Without horizontal and vertical stabilizers, a combat flying wing with high aspect-ratio has strong nonlinear dynamic feature, and use multiple control surfaces to realize multi-axis controls. Its flight control system must be able to handle nonlinearity and control redundancy problems. The six-degree-of-freedom (6-DOF) nonlinear dynamics model of the flying wing is developed. Utilizing nonlinear dynamic inversion theory and control allocation technique, an advanced flight control system for the tracking of trajectory is designed. Numerical simulation results show that this flight control system could comparatively better solve the nonlinear control problem of such aircraft types.

Keywords—Flying wing, Aircraft, Dynamic inversion, Control allocation, Trajectory, Flight control, Nonlinear modeling, Simulation

I. INTRODUCTION

Next generation military aircrafts will require low radar cross section (RCS) characteristic. Flying wing is an ideal configuration nearly invisible to radar. However, the flying wing has the characteristics of degraded multi-axis stabilities, strong nonlinear dynamic feature, and control redundancy. In order to solve the problems of nonlinearity and the number of control surfaces exceeding the control commands, a flight trajectory control system with control allocation is designed using nonlinear dynamic inversion approach. The results can be used for reference in the design phase of flight control system for such novel configuration aircraft types.

II. AIRCRAFT DESCRIPTION

The aircraft chosen for study is a combat flying wing with high aspect-ratio [1]. It can perform missions of bombing, transport and reconnaissance, etc. For such military missions, it requires more precise trajectory control. As illustrated in Fig.1, the aircraft is being proposed with a large number of control surfaces, including elevons and split drag rudders.

Inboard elevons (IE) and outboard elevons (OE) are used for roll or pitch control, and their position limits are $-25^{\circ}\sim 25^{\circ}$. Split drag rudders (SDR) can fulfill yaw control with roll and pitch coupling effects, and their position limits are $0^{\circ}\sim 90^{\circ}$.

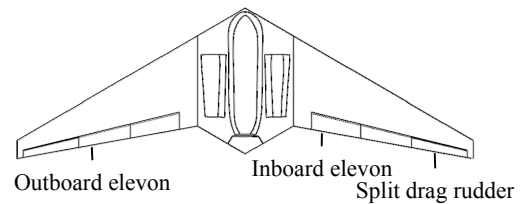


Figure 1. Configuration and control surfaces of flying wing

III. NONLINEAR DYNAMICS MODEL

It is assumed that: the aircraft is rigid-body; the Earth is treated as flat and stationary in inertial space [2]. The six-degree-of-freedom nonlinear dynamics model of the combat flying wing can be presented as follows [3], [4].

where, V , χ and γ denote respectively flight speed, flight path angle and heading angle; p , q and r denote respectively roll rate, pitch rate and yaw rate; α , β and μ denote respectively angle of attack, sideslip angle and velocity bank angle; X , Y and Z denote three components of aerodynamic force in aerodynamic axes; T_x , T_y and T_z denote three components of engine thrust in body axes; L , M and N denote respectively rolling moment, pitching moment and yawing moment; F_y and F_z are two components of total external force about O_{ya} axis and O_{za} axis in aerodynamic axes; m denotes mass of aircraft; I_x , I_y and I_z denote respectively moment of inertia in roll, pitch and yaw; I_{xz} denotes product of inertia about O_{xb} and O_{zb} axis in body axes.

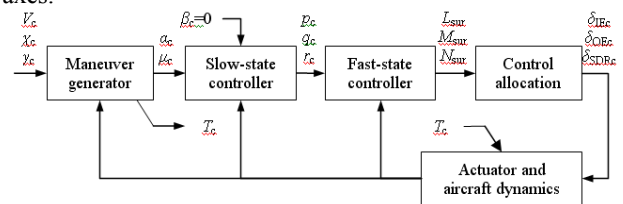


Figure 2. Block diagram of flight trajectory control system

IV. FLIGHT TRAJECTORY CONTROL SYSTEM

The basic structure of the flight trajectory control system mainly based on nonlinear dynamic inversion ([3], [4]) is shown in Fig.2. The control system has three inversion controllers and one control allocation block. The system command is velocity vector $(V_c \ \chi_c \ \gamma_c)T$. Thrust comand T_c

and control moments commands (Lsur Msur Nsur)T can be obtained through the three inversion controllers. Then deflection commands of control surfaces (δIEc δOEc δIEc)T can be obtained via the control allocation.

(1) Maneuver generator

Usually, sideslip is not expected in the maneuver, so keep β close to 0°. Thus, the point-mass equations can be simplified as follows.

$$\left. \begin{aligned} \dot{V} &= \frac{1}{m}[-X + (Y + T_x)\sin\beta - mg\sin\gamma + T_x\cos\beta\cos\alpha + T_x\cos\beta\sin\alpha] \\ \dot{\chi} &= \frac{1}{mV\cos\gamma}[Z\sin\mu + (Y + T_x)\cos\mu\cos\beta + T_x(\sin\mu\sin\alpha - \cos\mu\sin\beta\cos\alpha)] \\ &\quad - \frac{1}{mV\cos\gamma}[T_x(\cos\mu\sin\beta\sin\alpha + \sin\mu\cos\alpha)] \\ \dot{\gamma} &= \frac{1}{mV}[Z\cos\mu - mg\cos\gamma - (Y + T_x)\sin\mu\cos\beta + T_x(\sin\mu\sin\beta\cos\alpha + \cos\mu\sin\alpha)] \\ &\quad + \frac{1}{mV}[T_x(\sin\mu\sin\beta\sin\alpha - \cos\mu\cos\alpha)] \end{aligned} \right\} (1)$$

$$\left. \begin{aligned} \dot{p} &= \frac{I_x L + I_{xz} N + I_{xz}(I_x - I_y + I_z)pq + [I_x(I_y - I_z) - I_{xz}^2]qr}{I_x I_z - I_{xz}^2} \\ \dot{q} &= \frac{M + (I_z - I_x)pr + I_{xz}(r^2 - p^2)}{I_y} \\ \dot{r} &= \frac{I_{xz} L + I_x N + [I_x(I_x - I_y) + I_{xz}^2]pq + [I_{xz}(I_y - I_x - I_z)]qr}{I_x I_z - I_{xz}^2} \end{aligned} \right\} (2)$$

$$\left. \begin{aligned} \dot{\alpha} &= -p\cos\alpha\tan\beta + q - r\sin\alpha\tan\beta + F_z \sec\beta / (mV) \\ \dot{\beta} &= p\sin\alpha - r\cos\alpha + F_y / mV \\ \dot{\mu} &= p\cos\alpha\sec\beta + r\sin\alpha\sec\beta - F_z \tan\beta / (mV) \end{aligned} \right\} (3)$$

$$\left. \begin{aligned} \dot{V} &= \frac{1}{m}(T\cos\alpha - X - mg\sin\gamma) \\ \dot{\chi} &= \frac{1}{mV\cos\gamma}(T\sin\alpha\sin\mu + Z\sin\mu) \\ \dot{\gamma} &= \frac{1}{mV}(T\sin\alpha\cos\mu + Z\cos\mu - mg\cos\gamma) \end{aligned} \right\} (4)$$

The desired velocity dynamics are given as follows.

$$\left(\begin{array}{c} \dot{V}_c \\ \dot{\chi}_c \\ \dot{\gamma}_c \end{array} \right) = \left(\begin{array}{c} \omega_V (V_c - V) \\ \omega_\chi (\chi_c - \chi) \\ \omega_\gamma (\gamma_c - \gamma) \end{array} \right) \quad (5)$$

where ωV, ωχ and ωγ, are the respective bandwidths for three loops. Here, ωV=0.2rad/s, ωχ=ωγ=0.5rad/s.

From Eq.X(4)X, we can obtain thrust command Tc and aerodynamic angle commands αc, μc. The required velocity bank angle μc is obtained as follow.

$$\mu_c = \arctan\left(\frac{V\dot{\chi}_c \cos\gamma}{V\dot{\gamma}_c + g\cos\gamma}\right) \quad (6)$$

Then αc and Tc are obtained from Eq.X(4)X through Newton iteration algorithm.

(2) Slow-state controller

The desired dynamics of αc, βc and μc are as follows.

$$\left(\begin{array}{c} \dot{\alpha}_c \\ \dot{\beta}_c \\ \dot{\mu}_c \end{array} \right) = \left(\begin{array}{c} \omega_\alpha (\alpha_c - \alpha) \\ \omega_\beta (\beta_c - \beta) \\ \omega_\mu (\mu_c - \mu) \end{array} \right) \quad (7)$$

Here, ωα=ωβ=ωμ=2rad/s.

The desired angular velocities can be yielded as follows.

$$\left(\begin{array}{c} p_c \\ q_c \\ r_c \end{array} \right) = g^{-1} \left[\left(\begin{array}{c} \dot{\alpha}_c \\ \dot{\beta}_c \\ \dot{\mu}_c \end{array} \right) - f \right] \quad (8)$$

$$g = \begin{pmatrix} -\cos\alpha\tan\beta & 1 & -\sin\alpha\tan\beta \\ \sin\alpha & 0 & -\cos\alpha \\ \cos\alpha\sec\beta & 0 & \sin\alpha\sec\beta \end{pmatrix}, \quad \text{and}$$

where,

$$f = \frac{1}{m} \begin{pmatrix} F_z \sec\beta / V \\ F_y / V \\ -F_z \tan\beta / V \end{pmatrix} \quad (9)$$

(3) Fast-state controller

The desired dynamics of pc, qc and rc are as follows.

$$\left(\begin{array}{c} \dot{p}_c \\ \dot{q}_c \\ \dot{r}_c \end{array} \right) = \left(\begin{array}{c} \omega_p (p_c - p) \\ \omega_q (q_c - q) \\ \omega_r (r_c - r) \end{array} \right)$$

Here, ωp=ωq=ωr=10rad/s.

Then, the desired total external moments (Lc Mc Nc)T in body axes can be yielded as follows.

$$\left. \begin{aligned} L_c &= I_x \dot{p}_c + (I_z - I_y)qr - I_{xz}(pq + \dot{r}_c) \\ M_c &= I_y \dot{q}_c + (I_x - I_z)rp + I_{xz}(p^2 - r^2) \\ N_c &= I_z \dot{r}_c + (I_y - I_x)pq - I_{xz}(qr - \dot{p}_c) \end{aligned} \right\} (10)$$

Subtract body aerodynamic moments from total moments, the desired control moments (Lsur Msur Nsur)T can be yielded as follows.

$$\left. \begin{aligned} L_{sur} &= L_c - (L_\beta\beta + L_p p + L_r r) \\ M_{sur} &= M_c - (M_0 + M_\alpha\alpha + M_{\dot{\alpha}}\dot{\alpha} + M_q q) \\ N_{sur} &= N_c - (N_\beta\beta + N_p p + N_r r) \end{aligned} \right\} (11)$$

where the subscript “sur” represents control surfaces.

(4) Control allocation

The control surface deflection commands can be obtained through control allocation. Control allocation takes into account kinds of optimization objectives. Here, the optimization objective of minimum additional drag generated by control surfaces is considered [5].

$$\min J = \Delta C_D(u) \quad (12)$$

where, u=(δIElc δIErc δOElc δOErc δSDRlc δSDRrc)T denotes control vector; “l” and “r” represent respectively left and right side control surface; ΔCD(u) denotes the additional drag generated by control surfaces.

The constraint conditions are described as follows.

$$\left. \begin{aligned} g(u) &= M_d \\ u_{min} &\leq u \leq u_{max} \end{aligned} \right\} \quad (13)$$

where, Md denote the desired control moment vector; the first formula represents the command that control surfaces fulfill desired control moments; the second formula is deflection constraints of control surfaces.

Finally, subjected to the constraints of Eq.(13), the deflection command of every control surface is solved through some optimization algorithms.

V. SIMULATION AND ANALYSIS

The simulation is implementing on the 6-DOF nonlinear dynamics model of the combat flying wing with high aspect-ratio. It starts at an initial condition of altitude $H=10000\text{m}$, velocity $V=150\text{m/s}$, in straight and level flight. The trajectory control mission is: the aircraft maneuvers to a steady climbing turn of constant velocity, heading angle $\chi=-40^\circ$ and flight path angle $\gamma=10^\circ$. Simulation curves are shown in Figs.3-6.

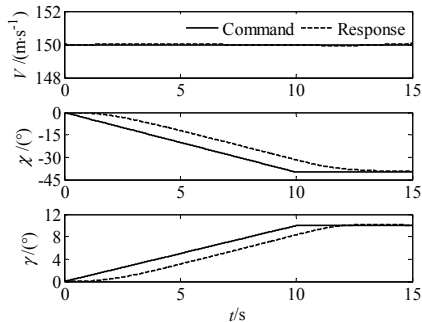


Figure 3. Response curve of velocity vector

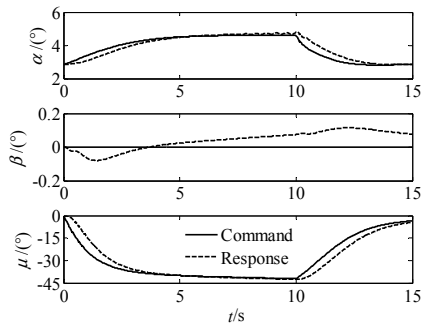


Figure 4. Response curves of aerodynamic angles

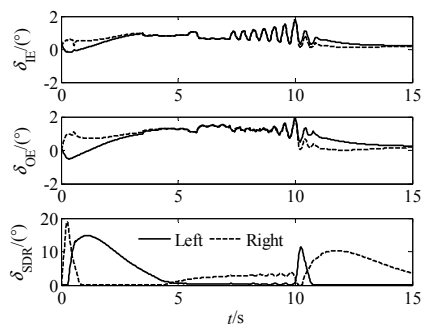


Figure 5. Response curves of control surfaces

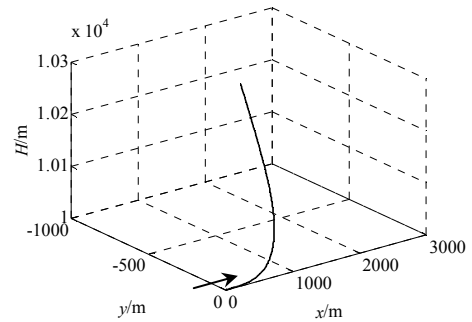


Figure 6. Aircraft flight trajectory

As Figs.3-4 indicate, the aircraft tracks the commands very well. Fig.5 shows that each control surface deflects in the constraint range. As can be seen in Fig.6, the aircraft performs a climbing turn task. Response curves show that the flight trajectory control system exhibits excellent tracking performance.

VI. SUMMARIES

Using nonlinear dynamic inversion and control allocation, an advanced flight trajectory control system of a combat flying wing with high aspect-ratio is designed. Simulation results demonstrate that nonlinear dynamic inversion is a better method to solve the nonlinear control problem of the flying wing.

REFERENCES

- [1] MA Chao; LI Lin; WANG Li-xin. Design of Innovative Control Surfaces of Flying Wing Aircrafts with Large Ratio Aspect. Journal of Beijing University of Aeronautics and Astronautics[J], 2007, PP: 149-153.
- [2] Etkin B; Reid L D. Dynamics of Flight: Stability and Control. John Wiley & Sons, Inc.[M], 1996.
- [3] Snell S A; Enns D F; Garrard W L. Nonlinear Inversion Flight Control for a Supermaneuverable Aircraft. Journal of Guidance, Control, and Dynamics[J], 1992, PP: 976-984.
- [4] Snell S A. Nonlinear Dynamic-inversion Flight Control of Supermaneuverable Aircraft. University of Minnesota[D], 1991.
- [5] WANG Lei; WANG Li-xin; JIA Zhong-ren. Control Allocation Method for Combat Flying Wing with Multiple Control Surfaces. Acta Aeronautica et Astronautica Sinica[J], 2011, PP: 571-579.